Skeletal Radiol (2010) 39:473–480
DOI 10.1007/s00256-009-0844-1

SCIENTIFIC ARTICLE

Articular cartilage and labral lesions of the glenohumeral joint: diagnostic performance of 3D water-excitation true FISP MR arthrography

Tobias Johannes Dietrich · Marco Zanetti · Nadja Saupe · Christian W. A. Pfirrmann · Sandro F. Fucentese · Juerg Hodler

Received: 16 September 2009 / Revised: 19 November 2009 / Accepted: 23 November 2009 / Published online: 17 December 2009
© ISS 2009

Abstract
Objective To evaluate the diagnostic performance of MR arthrography in the detection of articular cartilage and labral lesions of the glenohumeral joint using a transverse 3D water-excitation true fast imaging with steady-state precession (FISP) sequence.
Materials and Methods Seventy-five shoulders were included retrospectively. Shoulder arthroscopy was performed within 6 months of MR arthrography. MR images were evaluated separately by two radiologists. They were blinded to clinical and arthroscopic information. Arthroscopy served as the reference standard.
Results For the detection of humeral cartilage lesions, sensitivities and specificities were 86% (12/14)/89% (50/56) for observer 1 and 93%/86% for observer 2) for the transverse true FISP sequence and 64%/86% (50%/82% for observer 2) for the coronal intermediate-weighted spin-echo images. The corresponding values for the glenoidal cartilage were 60% (6/10)/88% (51/58) (80%/76% for observer 2) and 70%/86% (60%/74% for observer 2) respectively. For the detection of abnormalities of the anterior labrum (only assessed on true FISP images) the values were 94% (15/16)/84% (36/43) (88%/79% for observer 2). The corresponding values for the posterior labrum were 67% (8/12)/77% (36/47) (observer 2: 25%/74%). The kappa values for the grading of the humeral and glenoidal cartilage lesions were 0.81 and 0.55 for true FISP images compared with 0.49 and 0.43 for intermediate-weighted fast spin-echo images. Kappa values for true FISP evaluation of the anterior and posterior part of the labrum were 0.81 and 0.70.
Conclusion Transverse 3D true FISP MR arthrography images are useful for the difficult diagnosis of glenohumeral cartilage lesions and suitable for detecting labral abnormalities.

Keywords Arthrography · Magnetic resonance imaging · Shoulder joint · Cartilage · Sensitivity and specificity

T. J. Dietrich (✉) · M. Zanetti · N. Saupe · C. W. A. Pfirrmann · J. Hodler
Department of Radiology,
Orthopedic University Hospital Balgrist,
Forchstrasse 340,
8008 Zurich, Switzerland
e-mail: tobias.dietrich@gmx.de

S. F. Fucentese
Department of Orthopedic Surgery, Orthopedic University,
Hospital Balgrist,
8008 Zurich, Switzerland

Present Address:
T. J. Dietrich
Department of Radiology, Kantonsspital Muensterlingen,
PO Box 8596, Münsterlingen, Switzerland

Introduction

Diagnostic performance of MR imaging and MR arthrography is only moderate in the assessment of glenohumeral cartilage lesions [1–3], although a wide range of MR sequences is available for cartilage assessment [4, 5]. The three-dimensional (3D) water-excitation true fast imaging with steady-state precession (FISP) sequence has shown favorable results for cartilage assessment in the knee [6].

The true FISP sequence belongs to the group of balanced steady-state free precession (SSFP) techniques. Acronyms used by other manufacturers for balanced SSFP include

balanced FFE and FIESTA. Balanced SSFP offers the highest signal-to-noise ratio (SNR) per unit time compared with all other imaging sequences [7].

Based on encouraging experiences in the knee [6] the true FISP sequence was introduced into our shoulder MR protocol, mainly for the assessment of articular cartilage and the labrum. To our knowledge, the diagnostic performance of this sequence for shoulder abnormalities has not previously been presented in the English peer-reviewed literature.

Thus, the objective of this study was to evaluate the diagnostic performance of MR arthrography in the detection of articular cartilage and labral lesions of the glenohumeral joint using a transverse 3D water-excitation true FISP sequence.

Materials and methods

Patients

Seventy-five shoulders in 74 patients (33 women, 41 men, mean age 53.0 years, range: 21–83 years) were included in this retrospective study. The indications for MR arthrography were suspected rotator cuff tear in 42, impingement in 16, glenohumeral instability in 7, degenerative osteoarthritis of the acromioclavicular joint in 3 and of the glenohumeral joint in 1, degeneration of the biceps tendon anchor in 2, partial biceps tendon tear in 1, non-specific pain in 1, calcific tendinitis in 1, and frozen shoulder in 1. Inclusion criteria were:

1. Patients with shoulder arthroscopy performed between 1 January 2007 and 31 December 2007 at our hospital
2. Availability of a true FISP MR arthrography of the shoulder performed at our institution using a standardized imaging protocol up to 6 months prior to arthroscopy

Exclusion criteria were:

1. Age below 18 years
2. Surgery performed before imaging
3. Suspected neoplasm
4. Arthroscopic description of the labrum and cartilage not sufficient for the purpose of this investigation (Fig. 1)

These data were acquired by one of the authors (TJD) who was not involved in the following evaluations of the MR images. There were complete data concerning humeral cartilage in 70, glenoidal cartilage in 68, and the anterior and posterior labrum in 59 glenohumeral joints. The mean time between MR imaging and arthroscopy was 54 days (range: 0–181 days). The institutional review board responsible does not require approval for this type of investigation if patients have given permission for anonymized review of their medical data for scientific purposes before the imaging examination. All patients in this study granted permission.

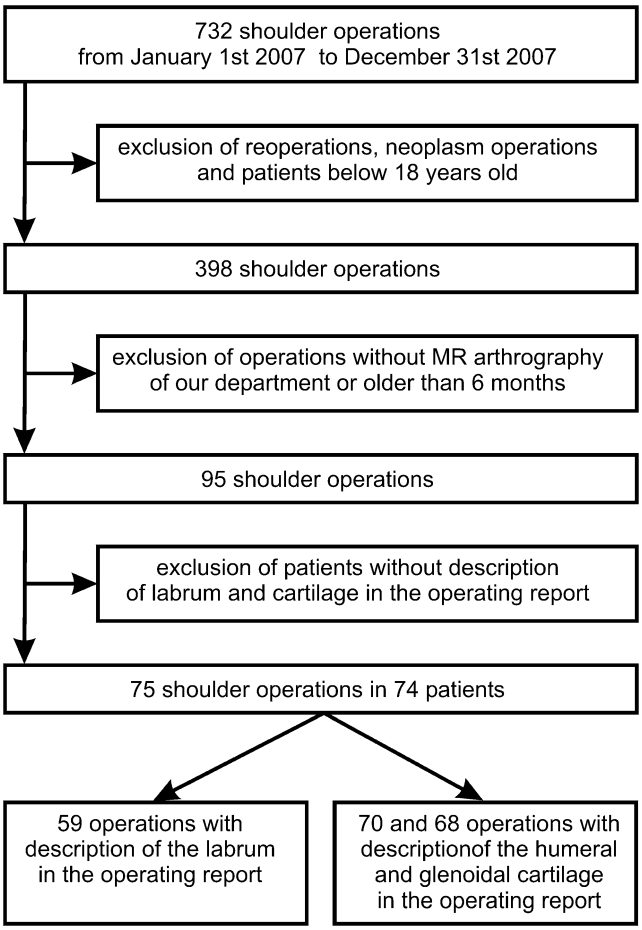

Fig. 1 Flow diagram of patient selection

Imaging protocol

All patients underwent MR imaging after fluoroscopically guided injection of 8–12 ml gadopentetate dimeglumine solution (Magnevist 2 mmol/l; Bayer Schering Pharma, Leverkusen, Germany) into the glenohumeral joint. The patients were examined in one of three different 1.5 Tesla MR units (Magnetom Symphony, Magnetom Espree and Magnetom Avanto, Siemens Medical Solutions, Erlangen, Germany), depending on scanner availability. The transverse 3D water-excitation true FISP and coronal intermediate-weighted (IW) fast spin-echo images with fat saturation MR arthrography sequences were acquired with the following parameters. Symphony; true FISP: repetition time ms (TR)/echo time ms (TE), 9.24/3.17; number of signals acquired (NSA), 1; field of view (FOV), 180×158 mm; matrix, 512×256; no interpolation; section

thickness, 1.7 mm, sections per slab, 48; flip angle, 28°; receiver bandwidth, 199 Hz/pixel; imaging time, 146 s; IW: TR/TE, 2,640/15; NSA, 1; FOV, 160×160 mm; matrix, 512×256; section thickness, 4.0 mm; sections per slab 19; receiver bandwidth, 130 Hz/pixel; turbo factor; 7; imaging time, 149 s; dedicated receive-only shoulder coil. Espree; true FISP: TR/TE, 12.43/5.31; NSA, 1; FOV, 180×180 mm; matrix, 512×256; no interpolation; section thickness, 1.7 mm, sections per slab, 48; flip angle, 28°; receiver bandwidth, 199 Hz/pixel; imaging time, 224 s; IW: TR/TE, 3,000/13; NSA, 1; FOV, 160×160 mm; matrix, 512×256; section thickness, 4.0 mm; sections per slab 19; receiver bandwidth, 130 Hz/pixel; turbo factor; 7; imaging time, 201 s; dedicated receive-only shoulder coil. Avanto; true FISP: TR/TE, 11.98/5.15; NSA, 1; FOV, 180×180 mm; matrix, 512×256; no interpolation; section thickness, 1.7 mm, sections per slab, 48; flip angle, 28°; receiver bandwidth, 199 Hz/pixel; imaging time, 216 s; IW: TR/TE, 2900/13; NSA, 1; FOV, 160×160; matrix, 512×256; section thickness, 4.0 mm; sections per slab 19; receiver bandwidth, 130 Hz/pixel; turbo factor; 7; imaging time, 194 s; dedicated receive-only shoulder coil.

Three additional sequences that were not evaluated in this investigation were also included in the routine MR arthrography protocol: Coronal T1-weighted fast spin-echo images with fat saturation (e.g., Avanto: TR/TE, 667/12; FOV, 160×160 mm; matrix, 512×256; section thickness, 3.0 mm), sagittal T1-weighted spin-echo images (e.g., Avanto: TR/TE, 450/12; FOV, 160×160 mm; matrix, 512×256; section thickness, 4.0 mm) , and sagittal T2-weighted fast spin-echo images with fat saturation (e.g., Avanto: TR/TE, 3,500/79; FOV, 160×160 mm; matrix, 512×256; section thickness, 4.0 mm).

Surgical procedure

Shoulder arthroscopy was performed by one of five orthopedic surgeons specializing in diseases of the shoulder. Arthroscopy was performed using standard portals allowing complete evaluation of both glenohumeral cartilage and the labrum.

Magnetic resonance evaluation

Two radiologists with 10 (CWAP) and 3 years' (NS) experience in a musculoskeletal medical imaging department separately evaluated the MR arthrography images. They were blinded to the arthroscopy report and clinical data. The observers first analyzed articular cartilage and the labrum on the transverse true FISP images. Nine months later, during a second session, coronal intermediate-weighted fast spin-echo images with fat saturation were evaluated (articular cartilage only). A classification system of three grades was used: normal, superficial, and deep cartilage lesions. Findings of superficial lesions included defects less than 50% of the cartilage thickness for arthroscopy and thinning, signal intensity alterations or irregular surface for MR imaging respectively. The central bare area of the glenoid was not separately classified and was reported as normal by observers 1 and 2 in our study. Determination of the central bare area of the glenoid was a smoothly marginated subcentimeter area of thinning of the central articular cartilage [8]. Cartilage defects with more than 50% of the cartilage thickness were considered to be deep cartilage lesions both during arthroscopy and on MR images [1]. The anterior and posterior labrum were evaluated separately. A classification system of three grades was applied: normal (including variants such as sublabral hole), labral degeneration, and labral tear. At MR imaging labral degeneration was diagnosed in the presence of signal abnormalities and rounded labrum.

Statistical analysis

One author (TJD) who was not involved in the evaluations compared the MR imaging findings with the surgical reports. Sensitivity, specificity, accuracy, and positive and negative predictive values were calculated. Interobserver agreement was assessed with statistics [9]. values between 0.81 and 1.00 were considered to represent very good agreement, 0.61 and 0.80 good agreement, 0.41 and 0.60 moderate agreement, 0.21 and 0.40 fair agreement, and less than 0.20 poor agreement. A software package (SPSS, version 16.0.1; SPSS, Chicago, IL, USA) was used for all statistical calculations.

Results

At arthroscopy, humeral cartilage lesions were observed in 14 out of 70 glenohumeral joints (frequency, 20%). Seven lesions were graded as superficial and seven as deep. There were glenoidal cartilage lesions in 10 out of 68 (15%) glenohumeral joints at arthroscopy. Seven lesions were superficial and three were deep. At arthroscopy anterior labral abnormalities were noted in 16 out of 59 glenohumeral joints (27%). Ten lesions were graded as degeneration and six as tears. Posterior labrum abnormalities were found in 12 out of 59 shoulders (20%), there was labral degeneration in nine and a tear in three joints.

Tables 1 and 2 summarize the diagnostic performance of the two observers. For the detection of all humeral cartilage lesions including superficial lesions, sensitivities, specificities, and accuracies were 86% (12/14)/89% (50/56)/89% (62/70) for observer 1 (93%/86%/87% for observer 2) for the transverse true FISP MR arthrography sequence (Figs. 2, 3 and 4) and 64% (9/14)/86% (48/56)/81% (57/70) (50%/

Table 1 Diagnostic performance of MR arthrography for cartilage lesions of the glenohumeral joint. *FISP* fast imaging with steady-state precession, *IW* intermediate-weighted, *FS* fast spin-echo, *Cor* coronal

	Humeral cartilage (*N*=70)				Glenoidal cartilage (*N*=68)			
	Observer 1 true FISP	Observer 2 true FISP	Observer 1 IW FS Cor	Observer 2 IW FS Cor	Observer 1 true FISP	Observer 2 true FISP	Observer 1 IW FS Cor	Observer 2 IW FS Cor
All cartilage lesions including superficial lesions								
True-positive cases	12	13	9	7	6	8	7	6
True-negative cases	50	48	48	46	51	44	50	43
False-positive cases	6	8	8	10	7	14	8	15
False-negative cases	2	1	5	7	4	2	3	4
Sensitivity (%)	86	93	64	50	60	80	70	60
Specificity (%)	89	86	86	82	88	76	86	74
Accuracy (%)	89	87	81	76	84	76	84	72
Positive predictive value (%)	67	62	53	41	46	36	47	29
Negative predictive value (%)	96	98	91	87	93	96	94	91
Deep cartilage lesions								
True-positive cases	6	6	4	3	3	3	1	1
True-negative cases	61	60	63	61	60	58	64	63
False-positive cases	2	3	0	2	5	7	1	2
False-negative cases	1	1	3	4	0	0	2	2
Sensitivity (%)	86	86	57	43	100	100	33	33
Specificity (%)	97	95	100	97	92	89	98	97
Accuracy (%)	96	94	96	91	93	90	96	94
Positive predictive value (%)	75	67	100	60	38	30	50	33
Negative predictive value (%)	98	98	95	94	100	100	97	97

82%/76% for observer 2) for the coronal IW fast spin-echo MR arthrography images. The corresponding values for all glenoidal cartilage lesions including superficial lesions (Figs. 5, 6) were 60% (6/10)/88% (51/58)/84% (57/68) (80%/76%/76% for observer 2) for the true FISP images and 70% (7/10)/86% (50/58)/84% (57/68) (60%/74%/72% for observer 2) for the coronal IW fast spin-echo sequence respectively. For solely deep humeral cartilage lesions, sensitivities, specificities, and accuracies were 86% (6/7)/ 97% (61/63)/ 96%(67/70) for observer 1 (86%/95%/94% for observer 2) for the true FISP MR arthrography images and 57% (4/7)/100% (63/63)/96% (67/70) (43%/97%/91% for observer 2) for the spin-echo images. The corresponding values for solely deep glenoidal cartilage lesions were 100% (3/3)/92% (60/65)/93% (63/68) (100%/89%/90% for observer 2) for the true FISP images and 33% (1/3)/98% (64/65)/96% (65/68) (33%/97%/94% for observer 2) for the coronal IW fast spin-echo sequence.

Labrum abnormalities were assessed exclusively on true FISP MR arthrography images. For the detection of all abnormalities of the anterior labrum including degeneration (Figs. 2, 7) sensitivities, specificities, and accuracies were 94% (15/16)/84% (36/43)/86% (51/59) for observer 1 (88%/79%/81% for observer 2). The corresponding values for all abnormalities of the posterior labrum including degeneration were 67% (8/12)/77% (36/47)/75% (44/59) for observer 1 (25%/74%/64% for observer 2). For tears of the anterior labrum sensitivities, specificities, and accuracies were 83% (5/6)/87% (46/53)/86% (51/59) for observer 1 (83%/ 89%88% for observer 2). For tears of the posterior labrum (Fig. 8) the values were 100% (3/3)/88% (49/56)/88% (52/59) for observer 1 (33%/89%/86% for observer 2).

The kappa values for the grading of the humeral and glenoidal cartilage lesions were 0.81 and 0.55 for true FISP images compared with 0.49 and 0.43 for IW fast spin-echo images (Tables 3, 4). Kappa values for true FISP evaluation of the anterior and posterior parts of the labrum were 0.81 and 0.70 respectively (Table 5). Differences among all three similar MR units were not observed, although there was no formal evaluation.

Discussion

The results of our study demonstrate a good diagnostic performance of true FISP MR arthrography for assessment of cartilage and labral lesions in the glenohumeral joint with moderate to very good interobserver agreement. In the

Table 2 Diagnostic performance of true FISP MR arthrography for labrum abnormalities of the glenohumeral joint

	Anterior labrum (*N*=59)		Posterior labrum (*N*=59)	
	Observer 1	Observer 2	Observer 1	Observer 2
All labral abnormalities including degeneration				
True-positive cases	15	14	8	3
True-negative cases	36	34	36	35
False-positive cases	7	9	11	12
False-negative cases	1	2	4	9
Sensitivity (%)	94	88	67	25
Specificity (%)	84	79	77	74
Accuracy (%)	86	81	75	64
Positive predictive value (%)	68	61	42	20
Negative predictive value (%)	97	94	90	80
Labral tears				
True-positive cases	5	5	3	1
True-negative cases	46	47	49	50
False-positive cases	7	6	7	6
False-negative cases	1	1	0	2
Sensitivity (%)	83	83	100	33
Specificity (%)	87	89	88	89
Accuracy (%)	86	88	88	86
Positive predictive value (%)	42	45	30	14
Negative predictive value (%)	98	98	100	96

diagnosis of cartilage lesions, the transverse true FISP sequence compares favorably with the coronal IW spin-echo images. Our results compare favorably with MR arthrography using spin-echo sequences published by Guntern et al. from our institution in 2003 [1]. Their imaging protocol included fat-suppressed coronal T1-weighted spin-echo, transverse, and sagittal T1-weighted spin-echo, coronal T2-weighted fast spin-echo and coronal intermediate-weighted fast spin-echo images. In the present study, accuracy for cartilage lesions varied between 76% and 96% for true FISP and between 72% and 96% for the spin-echo sequence compared with a range of 65% to 89% with the sequences employed by Guntern et al. [1].

Assessment of glenohumeral cartilage is challenging because it is thin and curved [10]. In comparison to standard spin-echo sequences, the 3D true FISP sequence is able to

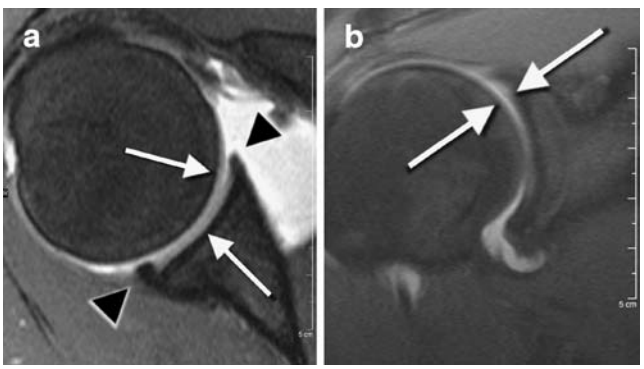

Fig. 2 Thirty-six-year-old woman with normal anterior and posterior labrum (*arrowheads*) and normal articular cartilage (*arrows*) of the right glenohumeral joint on **a** transverse true fast imaging with steady-state precession (FISP) and **b** coronal intermediate-weighted fast spin-echo with fat saturation arthrography images (true FISP; Siemens Symphony 1.5 T scanner: TR/TE, 9.24 ms/3.17 ms; flip angle, 28°. IW: TR/TE, 2,640/15)

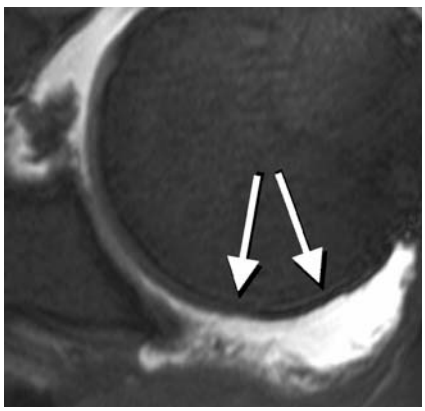

Fig. 3 Fifty-nine-year-old man with an arthroscopically proven superficial cartilage lesion (thinning less than 50% of the cartilage thickness) of the humeral cartilage (*arrows*) of the left glenohumeral joint. Note the subtle motion artifacts (transverse true FISP; Siemens Symphony 1.5T scanner: TR/TE, 9.24 ms/3.17 ms; flip angle, 28°)

Fig. 4 Seventy-five-year-old man with an arthroscopically proven deep articular cartilage lesion (full-thickness cartilage defect) of the humeral cartilage (*arrow*) of the left glenohumeral joint (transverse true FISP; Siemens Espree 1.5T scanner: TR/TE, 12.43 ms/5.31 ms; flip angle, 28°)

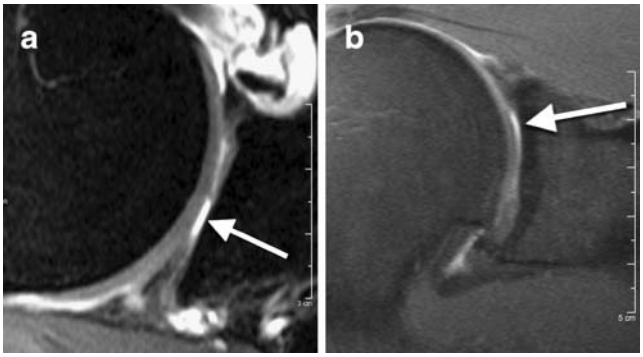

Fig. 6 Fifty-eight-year-old man with a deep articular cartilage lesion (full-thickness cartilage defect) of the glenoidal cartilage (*arrow*) of the right glenohumeral joint on **a** transverse true FISP and **b** coronal intermediate-weighted fast spin-echo with fat saturation arthrography images (true FISP; Siemens Symphony 1.5T scanner: TR/TE, 9.24 ms/3.17 ms; flip angle, 28°. IW: TR/TE, 2,640/15)

obtain contiguous sections in larger numbers (48 versus 19 according to our protocol), thinner slices (1.7 mm versus 4 mm) and provides higher SNR [5, 7, 11].

The thin and curved humeral cartilage and the thinner slices as well as the increased SNR of the true FISP sequence compared with spin-echo techniques may be responsible for the higher accuracy of superficial humeral cartilage lesions in the true FISP group [5]. General improvements in MR imaging quality over the past years, e.g., 1.0 Tesla MR unit in the study by Guntern et al. compared with the 1.5 Tesla MR unit in our study may in part be responsible for the higher accuracy in detecting cartilage lesions with the intermediate-weighted spin-echo images in the present study compared with that of Guntern et al. The 3D true FISP sequence also has disadvantages. Postoperative susceptibility artifacts associated with metallic implants are more pronounced in the true FISP than in standard T1-weighted or intermediate-weighted spin-echo sequences, which therefore retains an important role in postoperative imaging. In addition, the transverse 3D true FISP sequence has a longer acquisition time compared with the coronal intermediate-weighted fast spin-echo sequence applied in this investigation. However, the differences in acquisition time were not prohibitive for either sequence (3D true FISP/IW spin-echo: Symphony: 146/149 s, Espree: 224/201 s, and Avanto: 216/194 s).

The accuracy of 3D true FISP in detecting labral tears (86–88%) was comparable to previously reported results for

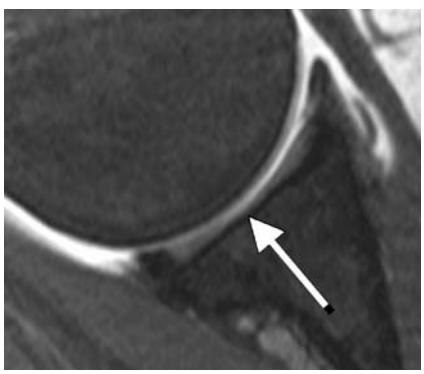

Fig. 5 Sixty-two-year-old man with a superficial lesion (thinning less than 50% of the cartilage thickness) of the glenoidal cartilage (*arrow*) of the right glenohumeral joint. The subtle distinction in MR arthrography of a superficial cartilage lesion and the central bare area [8] of the glenoid may be difficult. However, this lesion was classified as chondromalacia in the arthroscopic report (transverse true FISP; Siemens Symphony 1.5T scanner: TR/TE, 9.24 ms/3.17 ms; flip angle, 28°)

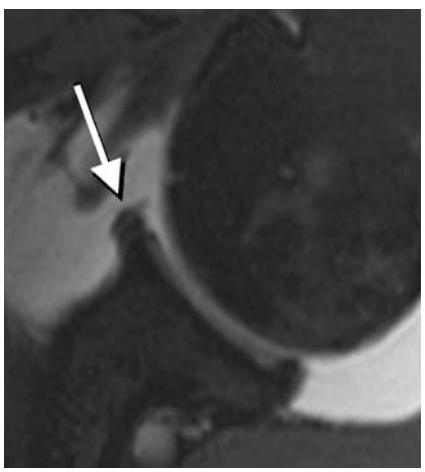

Fig. 7 Forty-five-year-old woman with arthroscopically proven degeneration (rounding and signal alteration) of the anterior labrum (*arrow*) of the left glenohumeral joint (transverse true FISP; Siemens Avanto 1.5T scanner: TR/TE, 11.98 ms/5.15 ms; flip angle, 28°)

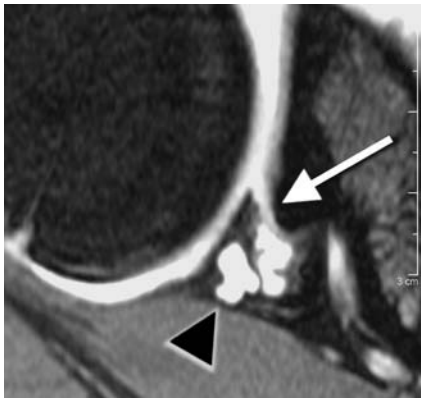

Fig. 8 Twenty-one-year-old man with a tear of the posterior labrum (*arrow*) and an associated labral cyst (*arrowhead*) of the right glenohumeral joint (transverse true FISP; Siemens Avanto 1.5T scanner: TR/TE, 11.98 ms/5.15 ms; flip angle, 28°)

spin-echo MR arthrography. Although there are far more papers evaluating the labrum than articular cartilage of the glenohumeral joint, our results cannot easily be compared with those in the literature, because of the different study designs, definition of labral abnormalities, and patient inclusion criteria. Waldt et al. [12] found an accuracy of 89% in the detection of labroligamentous injuries with T1- and T2-weighted spin-echo MR arthrography performed in three planes. Applegate et al. [13] excluded patients with acute injuries and reported an accuracy of 86% for chronic labral tears with spin-echo T1-weighted MR arthrography in three planes. Lee et al. [14] compared MR arthrography performed with a gradient echo sequence and a standard T1-weighted spin-echo sequence with regard to their diagnostic performance in labral tears. They found a significantly higher sensitivity (88% versus 64%; $p<0.05$), but slightly lower specificity for the gradient echo sequence. There is a marked difference in sensitivity of degeneration and tear of the posterior labrum between the two observers in our study. Labral degeneration may be difficult to differentiate from the numerous labral variants, as has been described before [15]. The frequency of posterior labrocapsular complex lesions after acute posterior shoulder dislocation was 58% in a previously published study [16]. However, only occasional labral tears were observed in other reports in patients with acute posterior shoulder dislocation [17, 18], indicating possible problems with the differentiation of degeneration or variants from symptomatic tears. The 3D true FISP sequence provides a T2-weighted component and thus demonstrates bursitis and bone marrow edema-like abnor-

Table 4 Interobserver agreement for the diagnosis and grading of articular cartilage lesions of the glenohumeral joint on coronal intermediate-weighted fast spin-echo images

Humeral cartilage, kappa=0.49

Findings for Observer 2	Findings for Observer 1			
	Normal	Superficial	Deep	Total
Normal	47	6	0	53
Superficial	5	6	1	12
Deep	1	1	3	5
Total	53	13	4	70

Glenoidal cartilage, kappa=0.43

Findings for Observer 2	Findings for Observer 1			
	Normal	Superficial	Deep	Total
Normal	43	3	1	47
Superficial	10	8	0	18
Deep	0	2	1	3
Total	53	13	2	68

Table 3 Interobserver agreement for the diagnosis and grading of articular cartilage lesions of the glenohumeral joint on transverse true FISP

Humeral cartilage, kappa=0.81

Findings for Observer 2	Findings for Observer 1			
	Normal	Superficial	Deep	Total
Normal	48	1	0	49
Superficial	4	8	0	12
Deep	0	1	8	9
Total	52	10	8	70

Glenoidal cartilage, kappa=0.55

Findings for Observer 2	Findings for Observer 1			
	Normal	Superficial	Deep	Total
Normal	45	1	0	46
Superficial	10	2	0	12
Deep	0	2	8	10
Total	55	5	8	68

Table 5 Interobserver agreement for the diagnosis and grading of labrum abnormalities of the glenohumeral joint on transverse true FISP

Anterior labrum, kappa=0.81

Findings for Observer 2	Findings for Observer 1			
	Normal	Degeneration	Tear	Total
Normal	34	0	2	36
Degeneration	3	9	0	12
Tear	0	1	10	11
Total	37	10	12	59

Posterior labrum, kappa=0.70

Findings for Observer 2	Findings for Observer 1			
	Normal	Degeneration	Tear	Total
Normal	38	3	3	44
Degeneration	2	6	0	8
Tear	0	0	7	7
Total	40	9	10	59

malities. However, this aspect was not tested in the current paper.

Our study had limitations. The retrospective study design is inferior to a prospective design with regard to the precision of arthroscopic reports. Based on the retrospective review of arthroscopic reports, no perfect comparison, for instance, by quadrants, was possible. However, only patients with arthroscopic reports sufficiently describing cartilage damage were included in our study (Fig. 1). During the time period of up to 6 months between MR arthrography and arthroscopy, new trauma may change the appearance of the labrum and cartilage. However, no intercurrent injury was detected during review of the electronic patient charts. A comparison of the transverse true FISP with a spin-echo sequence in the same plane may be superior to our study design with MR sequences obtained in two different imaging planes. The pear-shaped morphology of the glenoid might favor the use of the transverse imaging plane because of the higher sensitivity of lesions at the labral chondral junction compared with the coronal plane. On the other hand, the coronal plane provides better visualization of the superior articular surface of the humeral head.

The number of deep cartilage lesions in our study is relatively small, which limits the statistical analysis of the results. This might be explained by our study group. Most of our patients were referred for the assessment of rotator cuff tears and shoulder impingement. On the other hand the orthopedic surgeons of our hospital request CT arthrography in patients with suspected severe rotator cuff arthropathy to aid the treatment decision of reversed shoulder endoprostheses.

We conclude that transverse 3D true FISP MR arthrography images are useful for the difficult diagnosis of glenohumeral cartilage lesions and suitable for detecting labral abnormalities.

References

1. Guntern DV, Pfirrmann CW, Schmid MR, et al. Articular cartilage lesions of the glenohumeral joint: diagnostic effectiveness of MR arthrography and prevalence in patients with subacromial impingement syndrome. Radiology. 2003;226:165–70.
2. Yeh LR, Kwak S, Kim YS, et al. Evaluation of articular cartilage thickness of the humeral head and the glenoid fossa by MR arthrography: anatomic correlation in cadavers. Skeletal Radiol. 1998;27:500–4.
3. Hodler J, Loredo RA, Longo C, Trudell D, Yu JS, Resnick D. Assessment of articular cartilage thickness of the humeral head: MR-anatomic correlation in cadavers. AJR Am J Roentgenol. 1995;165:615–20.
4. Link TM, Stahl R, Woertler K. Cartilage imaging: motivation, techniques, current and future significance. Eur Radiol. 2007;17:1135–46.
5. Hargreaves BA, Gold GE, Beaulieu CF, Vasanawala SS, Nishimura DG, Pauly JM. Comparison of new sequences for high-resolution cartilage imaging. Magn Reson Med. 2003;49:700–9.
6. Duc SR, Pfirrmann CW, Schmid MR, et al. Articular cartilage defects detected with 3D water-excitation true FISP: Prospective comparison with sequences commonly used for knee imaging. Radiology. 2007;245:216–23.
7. Scheffler K, Lehnhardt S. Principles and applications of balanced SSFP techniques. Eur Radiol. 2003;13:2409–18.
8. Ly JQ, Bui-Mansfield LT, Kline MJ, DeBerardino TM, Taylor DC. Bare area of the glenoid: magnetic resonance appearance with arthroscopic correlation. J Comput Assist Tomogr. 2004;28:229–32.
9. Landis JR, Koch GG. An application of hierarchical kappa-type statistics in the assessment of majority agreement among multiple observers. Biometrics. 1977;33:363–74.
10. Graichen H, Jakob J, von Eisenhart-Rothe R, Englmeier KH, Reiser M, Eckstein F. Validation of cartilage volume and thickness measurements in the human shoulder with quantitative magnetic resonance imaging. Osteoarthritis Cartilage. 2003;11:475–82.
11. Andreisek G, Froehlich JM, Hodler J, et al. Direct MR Arthrography at 1.5 and 3.0 T: signal dependence on gadolinium and iodine concentrations—phantom study. Radiology. 2008;247:706–16.
12. Waldt S, Burkart A, Imhoff AB, Bruegel M, Rummeny EJ, Woertler K. Anterior shoulder instability: accuracy of MR Arthrography in the classification of anteroinferior labroligamentous injuries. Radiology. 2005;237:578–83.
13. Applegate GR, Hewitt M, Snyder SJ, Watson E, Kwak S, Resnick D. Chronic labral tears: value of magnetic resonance arthrography in evaluating the glenoid labrum and labral-bicipital complex. Arthroscopy. 2004;20:959–63.
14. Lee MJ, Motamedi K, Chow K, Seeger LL. Gradient-recalled echo sequences in direct shoulder MR arthrography for evaluating the labrum. Skeletal Radiol. 2008;37:19–25.
15. Zanetti M, Carstensen T, Weishaupt D, Jost B, Hodler J. MR arthrographic variability of the arthroscopically normal glenoid labrum: Qualitative and quantitative assessment. Eur Radiol. 2001;11:559–66.
16. Saupe N, White LM, Bleakney R, et al. Acute traumatic posterior shoulder dislocation: MR findings. Radiology. 2008;248:185–93.
17. Hottya GA, Tirman PF, Bost FW, Montgomery WH, Wolf EM, Genant HK. Tear of the posterior shoulder stabilizers after posterior dislocation: MR imaging and MR arthrographic findings with arthroscopic correlation. AJR Am J Roentgenol. 1998;171:763–8.
18. Cicak N. Posterior dislocation of the shoulder. J Bone Joint Surg Br. 2004;86:324–32.